



UNIVERSITY
OF TRENTO

DIPARTIMENTO DI INGEGNERIA E SCIENZA DELL'INFORMAZIONE

38123 Povo – Trento (Italy), Via Sommarive 14
<http://www.disi.unitn.it>

SYNTHESIS AND OPTIMIZATION OF PRE-FRACTAL
MULTIBAND ANTENNAS

R. Azaro, E. Zeni, M. Zambelli, and A. Massa

January 2011

Technical Report # DISI-11-247

SYNTHESIS AND OPTIMIZATION OF PRE-FRACTAL MULTIBAND ANTENNAS

R. Azaro, E. Zeni, M. Zambelli, and A. Massa

*Department of Information and Communication Technology
University of Trento, Via Sommarive 14, 38050 Trento, Italy
e-mail: andrea.massa@ing.unitn.it, Web-page: <http://www.eledia.ing.unitn.it>*

ABSTRACT

Nowadays electronic products often employ more than one wireless standards for data exchange, requiring the adoption of multi-band components and devices. In this framework in the paper the design of a monopolar dual-band antenna operating in the L_1 and L_2 GPS bands is presented. The pre-fractal geometry of the antenna has been synthesized by means of a Particle Swarm algorithm for optimizing the values of the electrical parameters within the specifications. In the paper some selected results of numerical simulations are shown and some comparisons between numerical and experimental data are presented.

1. INTRODUCTION

The growing demand of electronic products employing several wireless standards for data exchange, working in different frequency bands, requires the adoption of multi-band components and devices. In this framework one of the most critical issue is the design of the radiating device since the development of a single antenna working in two or more frequency bands and belonging to a limited geometry is, in general, an hard task.

Wire antennas (basically dipoles and monopoles) can work in several frequency bands corresponding to the resonances of the structure, but multiple working frequencies are strictly linked by harmonic relationships and, in addition, their electrical performances (VSWR and gain) vary with the considered resonant frequency. Classical techniques for the development of multiband wire antennas are based on the insertion of reactive loads in the antenna structure in order to obtain and allocate multiple resonant frequencies.

In recent years the problem has been faced also exploiting the properties of fractal geometries combined with an optimization algorithm in order to optimize both antenna geometry and loads values and positions [1] [2]. As a matter of fact, the use of fractal geometries or pre-fractal geometries (built with a finite number of fractal iterations) for antenna synthesis has been proven to be very useful in order to achieve enhanced bandwidth and miniaturization [3] and recently, some interesting applications have been presented in literature [4] [5]. However the insertion of additional circuitual elements in the antenna structure requires longer manufacturing times and some uncertainty on antenna performance may be introduced by the tolerances of lumped components values. In addition, also employing PCB technology an antenna structure made of only metal on dielectric slab is more solid than a circuit-like structure.

In order to overcome the insertion of lumped load in the antenna geometry to allocate generic working frequencies, some degrees of freedom can be added to the fractal geometry by perturbing the characteristic fractal parameters. The synthesis of a multi-band fractal antenna in the paper is faced as an optimization problem by minimizing a specific cost function written for the particular fractal structure considered. The optimization is carried out through a numerical procedure based on a Particle Swarm Optimizer (PSO) [6] [7], by optimizing only the parameters of the fractal geometry, without the insertion of any lumped load. In order to assess the effectiveness of the synthesis procedure, numerical and experimental results obtained with a dual-band GPS antenna are presented and discussed.

2. SYNTHESIS OF A PRE-FRACTAL DUAL-BAND ANTENNA

The design of the dual-band GPS monopolar antenna has been formulated in terms of an optimization problem by defining and imposing suitable constraints both on the gain values and about the impedance matching at the input port in the L_1 and L_2 frequency bands of the GPS system (centred at $f_{L2} = 1227.60$ MHz and $f_{L1} = 1575.42$ MHz, respectively). As far as the antenna for the GPS receiver is concerned, radiation characteristics that guarantee a hemi-spherical coverage have been assumed. Moreover, a Voltage Standing Wave Ratio (VSWR) lower than 1.8 in both the working frequency bands (i.e., a reflected power lower than 10 % of the incident power) has been required at the input port the antenna. Such constraints have been chosen taking into account the following specification of a commercial GPS receiver:

- (a) gain values greater than $G_{\min} = 3$ dB_i at $\theta = 0^\circ$ and greater than $G_{\min} = -4$ dB_i at $\theta = 70^\circ$ respectively,
- (b) maximum value of the VSWR equal to 2.0.

Since the first stage of each GPS receiving system is generally a low noise preamplifier because of the low intensity of the GPS signals at the earth surface, then a better impedance matching has been imposed by decreasing the maximum $VSWR$ value from 2.0 up to $VSWR_{\max} = 1.8$ in order to allow improved performances.

Concerning the geometrical constraints, the antenna has been also required to belong to a physical platform of dimensions $10 \times 16 \text{ cm}^2$. By considering a microstrip structure printed on a planar dielectric substrate, the parameters to be optimized were the fractal geometry and the width and the length of each fractal segment. As far as the general shape of the generating antenna is concerned, a Koch-like geometry derived from the Koch curve described in [1] and [4] has been used. According to the notation used in [1], the antenna has been generated from the Koch curve by repeatedly applying the so-called *Hutchinson operator* until the stage $i=2$, in order to obtain a radiating device having two resonant frequencies.

In general, the antenna structure at i -th stage is uniquely determined by:

- (a) a set of segment lengths $s_{i,j}$, i being the index of the fractal stage and j ($j = 1, \dots, 4^i$) indicates the j -th segment at the i -th stage,
- (b) a set of segment widths $w_{i,j}$,
- (c) a set of angles $\Theta_{h,q}$, $h = 1, \dots, 2^i$ and $q = 1, 2$ being $\Theta_{h,1} = \Theta_{h,2}$.

As an example, the descriptive parameters $s_{i,j}$ and $\Theta_{h,q}$ of the Koch-like curve at $i=1$ and $i=2$ are shown in Fig. 1(a) and in Fig. 1(b), respectively. In order to synthesize the GPS dual-band antenna, the $i=2$ stage has been considered and, in order to satisfy the project guidelines, the unknown descriptive parameters of the antenna have been optimized by minimizing the cost function Ω defined in terms of the least-square difference between requirements and estimated specifications:

$$\Omega(\underline{\gamma}) = \min[\varphi(\underline{\gamma}_i); i=2] \quad (1)$$

being

$$\begin{aligned} \varphi(\underline{\gamma}_i) = & \sum_{m=0}^{M-1} \sum_{n=0}^{N-1} \sum_{t=0}^{T-1} \left\{ \max \left[0, \frac{G_{\min}(t\Delta\theta, n\Delta\phi, m\Delta f) - \Phi(t\Delta\theta, n\Delta\phi, m\Delta f)}{G_{\min}} \right] \right\} + \\ & + \sum_{v=0}^{V-1} \left\{ \max \left[0, \frac{\Psi(v\Delta f) - VSWR_{\max}}{VSWR_{\max}} \right] \right\} \quad (2) \end{aligned}$$

where $\underline{\gamma}_i = \{s_{i,j}, w_{i,j}, \Theta_{h,1}; j=1, \dots, 4^i; h=1, \dots, 2^i\}$, Δf is the sampling frequency step in the L_1 and L_2 bands, $\Delta\theta$ and $\Delta\phi$ are the sampling angular steps of the gain

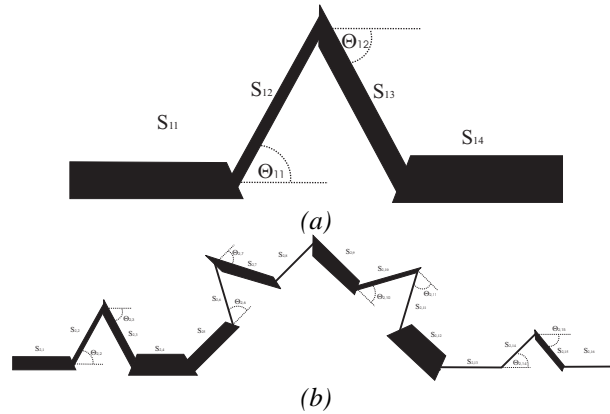


Figure 1. Descriptive parameters of the pre-fractal dual-band antenna: (a) $i=1$ and (b) $i=2$

function; $\Phi(\underline{\gamma}_i) = \Phi(t\Delta\theta, n\Delta\phi, m\Delta f)$ is the gain of the pre-fractal dual-band antenna evaluated at $\theta = t\Delta\theta$, $\phi = n\Delta\phi$, $f = m\Delta f$ and $\Psi(\underline{\gamma}_i) = \Psi(v\Delta f)$ is the $VSWR$ evaluated at the frequency $f = m\Delta f$ when the antenna structure is defined by the descriptive parameters array $\underline{\gamma}_i$, $i=2$. Besides the electrical constraints, suitable conditions

on the overall length and width of the fractal curve have been considered and a penalty has been imposed on some geometric configurations (e.g., having large ratio between width and length of the fractal segment) to avoid the generation of unfeasible structures.

In order to minimize (1) and according to the guidelines reported in [7], a suitable implementation of the PSO [8] has been integrated with a pre-fractal generator and a Method-of-Moments (MoM) [9] electromagnetic simulator. Starting from the set of trial arrays $\gamma_{-i,p}^{(k)}$ (i being the index of the considered fractal stage, i.e. $i=2$, p being the trial array index, $p=1,\dots,P$, and k the iteration index $k=1,\dots,K$, respectively) iteratively defined by the PSO, the pre-fractal generator defines the corresponding antenna structures for computing the corresponding $VSWR$ and gain values by means of the *MoM* simulator, which takes into account the presence of the dielectric slab and of the reference ground plane assumed of infinite extent. The iterative process continues until $k=K$ or $\Omega^{opt} \leq \eta$, η being the convergence threshold and $\Omega^{opt} = \min_k \left\{ \min_p \left[\Omega \left(\gamma_{-i,p}^{(k)} \right) \right] \right\}$.

3. NUMERICAL SYNTHESIS AND EXPERIMENTAL VALIDATION

The PSO implementation adopted in this work considers a population of $P=8$ trial solutions, a threshold

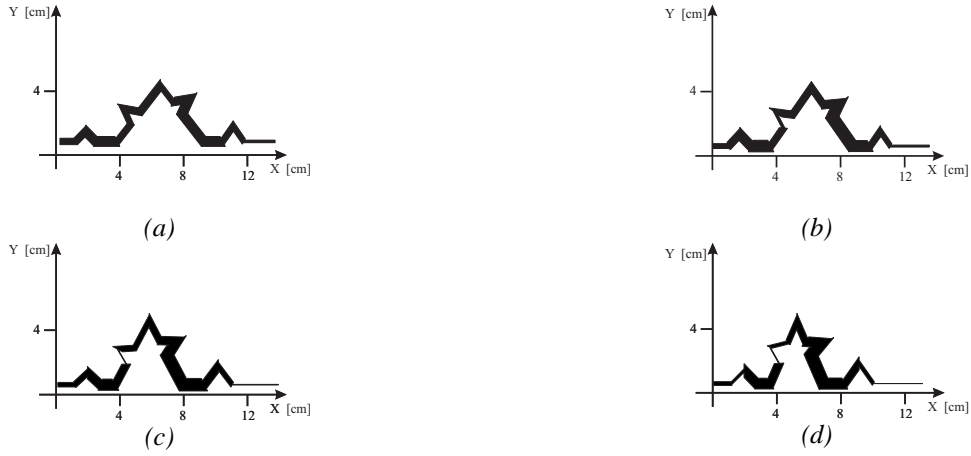


Figure 2. Geometry of the pre-fractal dual-band antenna during the optimization procedure: (a) $k=0$, (b) $k=10$, (c) $k=50$, (d), $k=k_{conv}$

$\eta=10^{-3}$, and a maximum number of iterations $K=2000$. The remaining parameters of the PSO have been set referring to the reference literature [7] and according to [8]. As an illustrative example of the iterative synthesis process, Figs. 2 and 3 show some representative processing results at various steps. At each optimization step, the structure of the best solution is shown (Fig. 2) as well as the plot of the corresponding *Return Loss (RL)* function (Fig. 3). As it can be observed, starting from a fully mismatched solution concerned with the structure displayed in Fig. 2(a) ($k=0$), the solution improves until the final geometry shown in Fig. 2(d) ($k=k_{conv}$) that fits the project specification in terms of both $VSWR$ values in L_1 and L_2 bands ($Return Loss < -11$ dB) and gain values at $\theta=0^\circ$ and $\theta=70^\circ$.

Furthermore, the synthesized antenna fits the geometrical constraints since its transversal and longitudinal dimensions are equal to 123 [mm] along the x-axis and 43 [mm] along the y-axis. Concerning the cost function minimization, Fig. 4 shows the plot of the cost function versus the iteration number. As it can be noticed, the optimization required $k_{conv}=367$ iterations and each iteration took an amount of CPU-time approximately of about 10 sec (Pentium IV 1800 MHz, 512 MB RAM).

As a result of the satisfactory numerical study, an experimental validation has been carried out. The antenna prototype has been built by using a photolithographic printing circuit technology following the geometric guidelines coming from the simulations and pictorially resumed in Fig. 2(d). As far as the $VSWR$ experimental measurements are concerned, the antenna prototype (Fig. 5) has been equipped with a *SMA* connector and it has been placed on a reference ground plane having dimensions equal to 90×140 cm^2 .

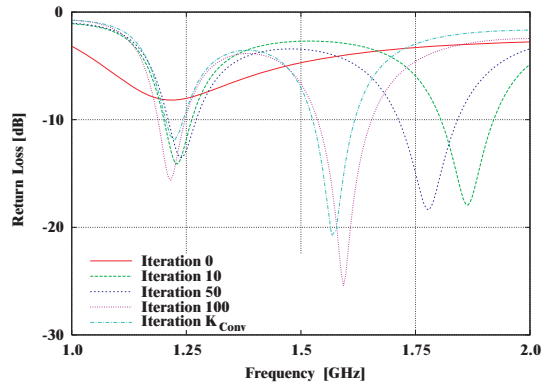


Figure 3. Simulated Return Loss values at the input port of the dual-band antenna during the optimization process

The Return Loss values have been measured with a scalar network analyzer by placing the antenna inside an anechoic chamber. Computed and measured Return Loss (RL) values have been compared and the results are shown in Fig. 6. As it can be observed, there is a good agreement between simulated and measured data, which satisfy the project constraints both in the L_1 band ($RL_{sim} = -20.63 \text{ dB}$ vs. $RL_{mis} = -28.3 \text{ dB}$) and in the L_2 band ($RL_{sim} = -11.8 \text{ dB}$ vs. $RL_{mis} = -15.4 \text{ dB}$).

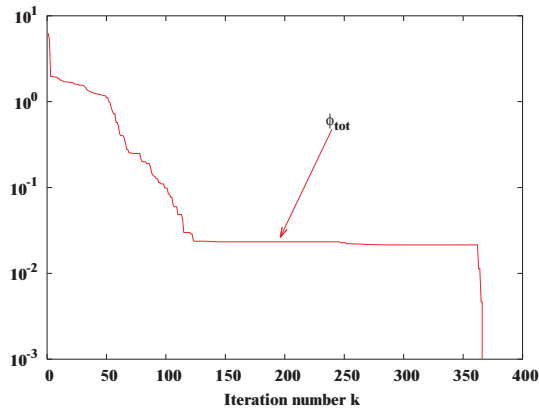


Figure 4. Behaviour of the Cost Function versus the iteration number



Figure 5. Photograph of the prototype of the GPS dual-band antenna

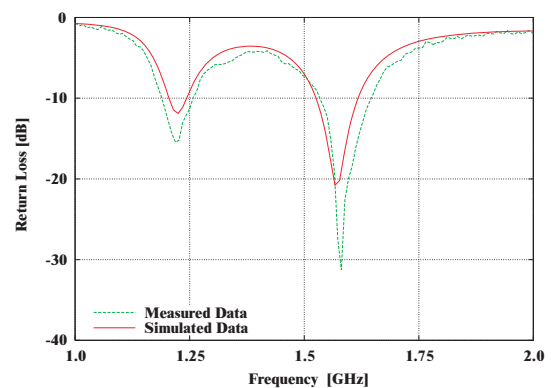


Figure 6. Pre-fractal dual-band GPS antenna: comparison between measured and simulated Return Loss values

In order to assess the effectiveness of the design methodology, the corresponding simulated and experimentally evaluated VSWR values are compared in Fig. 7 with those concerned with two quarter wave monopoles working in the L_1 and in the L_2 bands, and with the values reported in [10] for a GPS dual-band loaded antenna. Although the

synthesized structure presents a x-length equal to approximately $\lambda_2/2$, λ_2 being the wavelength at $f_{L2} = 1227.60 \text{ MHz}$, it gives *VSWR* values comparable with those of the corresponding quarter wave monopoles, but avoiding the use of multiple wired structures or a tuning circuit. Moreover, the *VSWR* behaviour turns out to be similar to that in [10] and concerned with a loaded antenna, but without lumped loads.

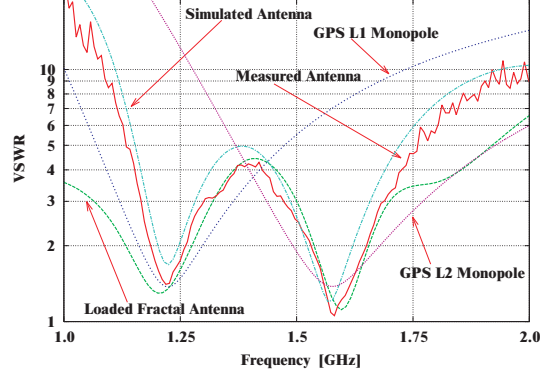


Figure 7. Pre-fractal dual-band GPS antenna: comparison between optimized antenna and standard quarter wave monopoles

Finally, Figs. 8(a)-(b) show the simulated gain functions in the horizontal plane ($\theta = 90^\circ$) and in a vertical plane ($\phi = 0^\circ$), respectively.

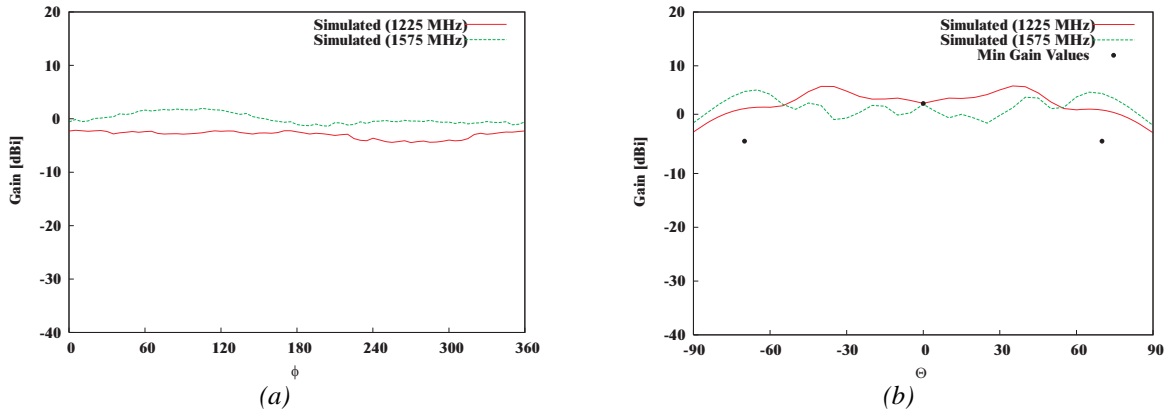


Figure 8. Pre-fractal dual-band GPS antenna: calculated gain functions at (a) the horizontal plane and (b) at a vertical plane ($\phi = 0^\circ$)

In order to validate the compliance to the requirements in a realistic configuration, the numerical simulations have been carried out considering a finite ground plane having the same dimensions of that used during *VSWR* measurements ($90 \times 140 \text{ cm}^2$). As expected, the synthesized antenna allows an hemispherical coverage requested by the GPS applications. Moreover the gain values at $\theta = 0^\circ$ and at $\theta = 70^\circ$ turn out to be greater than specifications ($\Phi(\theta = 0^\circ) > G_{\min}(\theta = 0^\circ) = 3.0 \text{ dB}_i$ and $\Phi(\theta = 70^\circ) > G_{\min}(\theta = 70^\circ) = -4.0 \text{ dB}_i$).

4. CONCLUSIONS

The design and optimization of a dual-band pre-fractal GPS antenna printed on a dielectric substrate has been described. The antenna structure has been synthesized through a suitable Particle Swarm algorithm by optimizing the descriptive parameters of a Kock-like pre-fractal geometry in order to comply with the geometrical requirements as well as the electrical constraints in the L_1 and L_2 GPS frequency bands. A prototype of the dual-band antenna has been built and some comparisons between measured and simulated *VSWR* values have been carried out in order to assess the effectiveness of the optimized antenna as well as of the synthesis procedure.

ACKNOWLEDGMENT

This work was in part supported in Italy by *Study and Development of Innovative Smart Systems for Highly Reconfigurable Mobile Networks*, Progetto di Ricerca di Interesse Nazionale - Miur Project COFIN 2005099984.

REFERENCES

1. D. H. Werner, P. L. Werner, and K. H. Church, "Genetically engineered multiband fractal antennas," *Electron. Lett.*, vol. 37, pp. 1150-1151, Sep. 2001.
2. D. H. Werner and R. Mittra, *Frontiers in electromagnetics*. Piscataway: IEEE Press, 2000.
3. J. Gianvittorio and Y. Rahmat-Samii, "Fractals antennas: A novel antenna miniaturization technique, and applications," *IEEE Antennas Propagat. Mag.*, vol. 44, pp. 20-36, Feb. 2002.
4. C. P. Baliarda, J. Romeu, and A. Cardama, "The Koch monopole: a small fractal antenna," *IEEE Antennas Propagat. Mag.*, vol. 48, pp. 1773-1781, Nov. 2000.
5. S. R. Best, "On the performance properties of the Koch fractal and other bent wire monopoles," *IEEE Trans. Antennas Propagat.*, vol. 51, pp. 1292-1300, Jun. 2003.
6. M. Donelli and A. Massa, "A computational approach based on a particle swarm optimizer for microwave imaging of two-dimensional dielectric scatterers," *IEEE Trans. Microwave Theory Techn.*, vol. 53, pp. 1761-1776, May 2005.
7. J. Robinson and Y. Rahmat-Samii, "Particle swarm optimization in electromagnetics," *IEEE Trans. Antennas Propagat.*, vol. 52, pp. 397-407, Feb. 2004.
8. R. Azaro, F. De Natale, M. Donelli, A. Massa, and E. Zeni, "Optimized design of a multi-function/multi-band antenna for automotive rescue systems," *IEEE Trans. Antennas Propagat. - Special Issue on "Multifunction Antennas and Antenna Systems*, vol. 54, pp. 394-400, Feb. 2006.
9. R. F. Harrington, *Field Computation by Moment Methods*. Malabar, Florida: Robert E. Krieger Publishing Co., 1987.
10. D. H. Werner and S. Ganguly, "An overview of fractal antenna engineering research," *IEEE Antennas Propagat. Mag.*, vol. 45, pp. 38-57, 2003.